

Model-independent search for the decay $B^+ \rightarrow l^+ \nu_l \gamma$

B. Aubert,¹ Y. Karyotakis,¹ J. P. Lees,¹ V. Poireau,¹ E. Prencipe,¹ X. Prudent,¹ V. Tisserand,¹ J. Garra Tico,² E. Grauges,² M. Martinelli,^{3a,3b} A. Palano,^{3a,3b} M. Pappagallo,^{3a,3b} G. Eigen,⁴ B. Stugu,⁴ L. Sun,⁴ M. Battaglia,⁵ D. N. Brown,⁵ L. T. Kerth,⁵ Yu. G. Kolomensky,⁵ G. Lynch,⁵ I. L. Osipenkov,⁵ K. Tackmann,⁵ T. Tanabe,⁵ C. M. Hawkes,⁶ N. Soni,⁶ A. T. Watson,⁶ H. Koch,⁷ T. Schroeder,⁷ D. J. Asgeirsson,⁸ B. G. Fulsom,⁸ C. Hearty,⁸ T. S. Mattison,⁸ J. A. McKenna,⁸ M. Barrett,⁹ A. Khan,⁹ A. Randle-Conde,⁹ V. E. Blinov,¹⁰ A. D. Bukin,^{10,*} A. R. Buzykaev,¹⁰ V. P. Druzhinin,¹⁰ V. B. Golubev,¹⁰ A. P. Onuchin,¹⁰ S. I. Serednyakov,¹⁰ Yu. I. Skovpen,¹⁰ E. P. Solodov,¹⁰ K. Yu. Todyshev,¹⁰ M. Bondioli,¹¹ S. Curry,¹¹ I. Eschrich,¹¹ D. Kirkby,¹¹ A. J. Lankford,¹¹ P. Lund,¹¹ M. Mandelkern,¹¹ E. C. Martin,¹¹ D. P. Stoker,¹¹ H. Atmacan,¹² J. W. Gary,¹² F. Liu,¹² O. Long,¹² G. M. Vitug,¹² Z. Yasin,¹² V. Sharma,¹³ C. Campagnari,¹⁴ T. M. Hong,¹⁴ D. Kovalskyi,¹⁴ M. A. Mazur,¹⁴ J. D. Richman,¹⁴ T. W. Beck,¹⁵ A. M. Eisner,¹⁵ C. A. Heusch,¹⁵ J. Kroseberg,¹⁵ W. S. Lockman,¹⁵ A. J. Martinez,¹⁵ T. Schalk,¹⁵ B. A. Schumm,¹⁵ A. Seiden,¹⁵ L. Wang,¹⁵ L. O. Winstrom,¹⁵ C. H. Cheng,¹⁶ D. A. Doll,¹⁶ B. Echenard,¹⁶ F. Fang,¹⁶ D. G. Hitlin,¹⁶ I. Narsky,¹⁶ P. Ongmongkolkul,¹⁶ T. Piatenko,¹⁶ F. C. Porter,¹⁶ R. Andreassen,¹⁷ G. Mancinelli,¹⁷ B. T. Meadows,¹⁷ K. Mishra,¹⁷ M. D. Sokoloff,¹⁷ P. C. Bloom,¹⁸ W. T. Ford,¹⁸ A. Gaz,¹⁸ J. F. Hirschauer,¹⁸ M. Nagel,¹⁸ U. Nauenberg,¹⁸ J. G. Smith,¹⁸ S. R. Wagner,¹⁸ R. Ayad,^{19,†} W. H. Toki,¹⁹ R. J. Wilson,¹⁹ E. Feltresi,²⁰ A. Hauke,²⁰ H. Jasper,²⁰ T. M. Karbach,²⁰ J. Merkel,²⁰ A. Petzold,²⁰ B. Spaan,²⁰ K. Wacker,²⁰ M. J. Kobel,²¹ R. Nogowski,²¹ K. R. Schubert,²¹ R. Schwierz,²¹ A. Volk,²¹ D. Bernard,²² E. Latour,²² M. Verderi,²² P. J. Clark,²³ S. Playfer,²³ J. E. Watson,²³ M. Andreotti,^{24a,24b} D. Bettoni,^{24a} C. Bozzi,^{24a} R. Calabrese,^{24a,24b} A. Cecchi,^{24a,24b} G. Cibinetto,^{24a,24b} E. Fioravanti,^{24a,24b} P. Franchini,^{24a,24b} E. Luppi,^{24a,24b} M. Munerato,^{24a,24b} M. Negrini,^{24a,24b} A. Petrella,^{24a,24b} L. Piemontese,^{24a} V. Santoro,^{24a,24b} R. Baldini-Ferrolì,²⁵ A. Calcaterra,²⁵ R. de Sangro,²⁵ G. Finocchiaro,²⁵ S. Pacetti,²⁵ P. Patteri,²⁵ I. M. Peruzzi,^{25,‡} M. Piccolo,²⁵ M. Rama,²⁵ A. Zallo,²⁵ R. Contri,^{26a,26b} E. Guido,^{26a,26b} M. Lo Vetere,^{26a,26b} M. R. Monge,^{26a,26b} S. Passaggio,^{26a} C. Patrignani,^{26a,26b} E. Robutti,^{26a} S. Tosi,^{26a,26b} K. S. Chaisanguanthum,²⁷ M. Morii,²⁷ A. Adametz,²⁸ J. Marks,²⁸ S. Schenk,²⁸ U. Uwer,²⁸ F. U. Bernlochner,²⁹ V. Klose,²⁹ H. M. Lacker,²⁹ D. J. Bard,³⁰ P. D. Dauncey,³⁰ M. Tibbetts,³⁰ P. K. Behera,³¹ M. J. Charles,³¹ U. Mallik,³¹ J. Cochran,³² H. B. Crawley,³² L. Dong,³² V. Eyges,³² W. T. Meyer,³² S. Prell,³² E. I. Rosenberg,³² A. E. Rubin,³² Y. Y. Gao,³³ A. V. Gritsan,³³ Z. J. Guo,³³ N. Arnaud,³⁴ J. Béquilleux,³⁴ A. D'Orazio,³⁴ M. Davier,³⁴ D. Derkach,³⁴ J. Firmino da Costa,³⁴ G. Grosdidier,³⁴ F. Le Diberder,³⁴ V. Lepeltier,³⁴ A. M. Lutz,³⁴ B. Malaescu,³⁴ S. Pruvot,³⁴ P. Roudeau,³⁴ M. H. Schune,³⁴ J. Serrano,³⁴ V. Sordini,^{34,§} A. Stocchi,³⁴ G. Wormser,³⁴ D. J. Lange,³⁵ D. M. Wright,³⁵ I. Bingham,³⁶ J. P. Burke,³⁶ C. A. Chavez,³⁶ J. R. Fry,³⁶ E. Gabathuler,³⁶ R. Gamet,³⁶ D. E. Hutchcroft,³⁶ D. J. Payne,³⁶ C. Touramanis,³⁶ A. J. Bevan,³⁷ C. K. Clarke,³⁷ F. Di Lodovico,³⁷ R. Sacco,³⁷ M. Sigamani,³⁷ G. Cowan,³⁸ S. Paramesvaran,³⁸ A. C. Wren,³⁸ D. N. Brown,³⁹ C. L. Davis,³⁹ A. G. Denig,⁴⁰ M. Fritsch,⁴⁰ W. Gradl,⁴⁰ A. Hafner,⁴⁰ K. E. Alwyn,⁴¹ D. Bailey,⁴¹ R. J. Barlow,⁴¹ G. Jackson,⁴¹ G. D. Lafferty,⁴¹ T. J. West,⁴¹ J. I. Yi,⁴¹ J. Anderson,⁴² C. Chen,⁴² A. Jawahery,⁴² D. A. Roberts,⁴² G. Simi,⁴² J. M. Tuggle,⁴² C. Dallapiccola,⁴³ E. Salvati,⁴³ R. Cowan,⁴⁴ D. Dujmic,⁴⁴ P. H. Fisher,⁴⁴ S. W. Henderson,⁴⁴ G. Sciolla,⁴⁴ M. Spitznagel,⁴⁴ R. K. Yamamoto,⁴⁴ M. Zhao,⁴⁴ D. M. Lindemann,⁴⁵ P. M. Patel,⁴⁵ S. H. Robertson,⁴⁵ M. Schram,⁴⁵ P. Biassoni,^{46a,46b} A. Lazzaro,^{46a,46b} V. Lombardo,^{46a} F. Palombo,^{46a,46b} S. Stracka,^{46a,46b} J. M. Bauer,⁴⁷ L. Cremaldi,⁴⁷ R. Godang,^{47,||} R. Kroeger,⁴⁷ P. Sonnek,⁴⁷ D. J. Summers,⁴⁷ H. W. Zhao,⁴⁷ M. Simard,⁴⁸ P. Taras,⁴⁸ H. Nicholson,⁴⁹ G. De Nardo,^{50a,50b} L. Lista,^{50a} D. Monorchio,^{50a,50b} G. Onorato,^{50a,50b} C. Sciacca,^{50a,50b} G. Raven,⁵¹ H. L. Snoek,⁵¹ C. P. Jessop,⁵² K. J. Knoepfel,⁵² J. M. LoSecco,⁵² W. F. Wang,⁵² L. A. Corwin,⁵³ K. Honscheid,⁵³ H. Kagan,⁵³ R. Kass,⁵³ J. P. Morris,⁵³ A. M. Rahimi,⁵³ J. J. Regensburger,⁵³ S. J. Sekula,⁵³ Q. K. Wong,⁵³ N. L. Blount,⁵⁴ J. Brau,⁵⁴ R. Frey,⁵⁴ O. Igonkina,⁵⁴ J. A. Kolb,⁵⁴ M. Lu,⁵⁴ R. Rahmat,⁵⁴ N. B. Sinev,⁵⁴ D. Strom,⁵⁴ J. Strube,⁵⁴ E. Torrence,⁵⁴ G. Castelli,^{55a,55b} N. Gagliardi,^{55a,55b} M. Margoni,^{55a,55b} M. Morandin,^{55a} M. Posocco,^{55a} M. Rotondo,^{55a} F. Simonetto,^{55a,55b} R. Stroili,^{55a,55b} C. Voci,^{55a,55b} P. del Amo Sanchez,⁵⁶ E. Ben-Haim,⁵⁶ G. R. Bonneaud,⁵⁶ H. Briand,⁵⁶ J. Chauveau,⁵⁶ O. Hamon,⁵⁶ Ph. Leruste,⁵⁶ G. Marchiori,⁵⁶ J. Ocariz,⁵⁶ A. Perez,⁵⁶ J. Prendki,⁵⁶ S. Sitt,⁵⁶ L. Gladney,⁵⁷ M. Biasini,^{58a,58b} E. Manoni,^{58a,58b} C. Angelini,^{59a,59b} G. Batignani,^{59a,59b} S. Bettarini,^{59a,59b} G. Calderini,^{59a,59b,||} M. Carpinelli,^{59a,59b,**} A. Cervelli,^{59a,59b} F. Forti,^{59a,59b} M. A. Giorgi,^{59a,59b} A. Lusiani,^{59a,59c} M. Morganti,^{59a,59b} N. Neri,^{59a,59b} E. Paoloni,^{59a,59b} G. Rizzo,^{59a,59b} J. J. Walsh,^{59a} D. Lopes Pegna,⁶⁰ C. Lu,⁶⁰ J. Olsen,⁶⁰ A. J. S. Smith,⁶⁰ A. V. Telnov,⁶⁰ F. Anulli,^{61a} E. Baracchini,^{61a,61b} G. Cavoto,^{61a} R. Faccini,^{61a,61b} F. Ferrarotto,^{61a} F. Ferroni,^{61a,61b} M. Gaspero,^{61a,61b} P. D. Jackson,^{61a} L. Li Gioi,^{61a} M. A. Mazzoni,^{61a} S. Morganti,^{61a} G. Piredda,^{61a} F. Renga,^{61a,61b} C. Voena,^{61a} M. Ebert,⁶² T. Hartmann,⁶² H. Schröder,⁶² R. Waldi,⁶² T. Adye,⁶³ B. Franek,⁶³ E. O. Olaiya,⁶³ F. F. Wilson,⁶³ S. Emery,⁶⁴ L. Esteve,⁶⁴ G. Hamel de Monchenault,⁶⁴ W. Kozanecki,⁶⁴ G. Vasseur,⁶⁴ Ch. Yèche,⁶⁴ M. Zito,⁶⁴ M. T. Allen,⁶⁵ D. Aston,⁶⁵ R. Bartoldus,⁶⁵ J. F. Benitez,⁶⁵

R. Cenci,⁶⁵ J. P. Coleman,⁶⁵ M. R. Convery,⁶⁵ J. C. Dingfelder,⁶⁵ J. Dorfan,⁶⁵ G. P. Dubois-Felsmann,⁶⁵ W. Dunwoodie,⁶⁵ R. C. Field,⁶⁵ M. Franco Sevilla,⁶⁵ A. M. Gabareen,⁶⁵ M. T. Graham,⁶⁵ P. Grenier,⁶⁵ C. Hast,⁶⁵ W. R. Innes,⁶⁵ J. Kaminski,⁶⁵ M. H. Kelsey,⁶⁵ H. Kim,⁶⁵ P. Kim,⁶⁵ M. L. Kocian,⁶⁵ D. W. G. S. Leith,⁶⁵ S. Li,⁶⁵ B. Lindquist,⁶⁵ S. Luitz,⁶⁵ V. Luth,⁶⁵ H. L. Lynch,⁶⁵ D. B. MacFarlane,⁶⁵ H. Marsiske,⁶⁵ R. Messner,^{65,*} D. R. Muller,⁶⁵ H. Neal,⁶⁵ S. Nelson,⁶⁵ C. P. O'Grady,⁶⁵ I. Ofte,⁶⁵ M. Perl,⁶⁵ B. N. Ratcliff,⁶⁵ A. Roodman,⁶⁵ A. A. Salnikov,⁶⁵ R. H. Schindler,⁶⁵ J. Schwiening,⁶⁵ A. Snyder,⁶⁵ D. Su,⁶⁵ M. K. Sullivan,⁶⁵ K. Suzuki,⁶⁵ S. K. Swain,⁶⁵ J. M. Thompson,⁶⁵ J. Va'vra,⁶⁵ A. P. Wagner,⁶⁵ M. Weaver,⁶⁵ C. A. West,⁶⁵ W. J. Wisniewski,⁶⁵ M. Wittgen,⁶⁵ D. H. Wright,⁶⁵ H. W. Wulsin,⁶⁵ A. K. Yarritu,⁶⁵ C. C. Young,⁶⁵ V. Ziegler,⁶⁵ X. R. Chen,⁶⁶ H. Liu,⁶⁶ W. Park,⁶⁶ M. V. Purohit,⁶⁶ R. M. White,⁶⁶ J. R. Wilson,⁶⁶ P. R. Burchat,⁶⁷ A. J. Edwards,⁶⁷ T. S. Miyashita,⁶⁷ S. Ahmed,⁶⁸ M. S. Alam,⁶⁸ J. A. Ernst,⁶⁸ B. Pan,⁶⁸ M. A. Saeed,⁶⁸ S. B. Zain,⁶⁸ A. Soffer,⁶⁹ S. M. Spanier,⁷⁰ B. J. Wogslund,⁷⁰ R. Eckmann,⁷¹ J. L. Ritchie,⁷¹ A. M. Ruland,⁷¹ C. J. Schilling,⁷¹ R. F. Schwitters,⁷¹ B. C. Wray,⁷¹ B. W. Drummond,⁷² J. M. Izen,⁷² X. C. Lou,⁷² F. Bianchi,^{73a,73b} D. Gamba,^{73a,73b} M. Pelliccioni,^{73a,73b} M. Bomben,^{74a,74b} L. Bosisio,^{74a,74b} C. Cartaro,^{74a,74b} G. Della Ricca,^{74a,74b} L. Lanceri,^{74a,74b} L. Vitale,^{74a,74b} V. Azzolini,⁷⁵ N. Lopez-March,⁷⁵ F. Martinez-Vidal,⁷⁵ D. A. Milanes,⁷⁵ A. Oyanguren,⁷⁵ J. Albert,⁷⁶ Sw. Banerjee,⁷⁶ B. Bhuyan,⁷⁶ H. H. F. Choi,⁷⁶ K. Hamano,⁷⁶ G. J. King,⁷⁶ R. Kowalewski,⁷⁶ M. J. Lewczuk,⁷⁶ I. M. Nugent,⁷⁶ J. M. Roney,⁷⁶ R. J. Sobie,⁷⁶ T. J. Gershon,⁷⁷ P. F. Harrison,⁷⁷ J. Ilic,⁷⁷ T. E. Latham,⁷⁷ G. B. Mohanty,⁷⁷ E. M. T. Puccio,⁷⁷ H. R. Band,⁷⁸ X. Chen,⁷⁸ S. Dasu,⁷⁸ K. T. Flood,⁷⁸ Y. Pan,⁷⁸ R. Prepost,⁷⁸ C. O. Vuosalo,⁷⁸ and S. L. Wu⁷⁸

(BABAR Collaboration)

¹Laboratoire d'Annecy-le-Vieux de Physique des Particules (LAPP), Université de Savoie, CNRS/IN2P3, F-74941 Annecy-Le-Vieux, France

²Universitat de Barcelona, Facultat de Física, Departament ECM, E-08028 Barcelona, Spain

^{3a}INFN Sezione di Bari, I-70126 Bari, Italy

^{3b}Dipartimento di Fisica, Università di Bari, I-70126 Bari, Italy

⁴University of Bergen, Institute of Physics, N-5007 Bergen, Norway

⁵Lawrence Berkeley National Laboratory and University of California, Berkeley, California 94720, USA

⁶University of Birmingham, Birmingham, B15 2TT, United Kingdom

⁷Ruhr Universität Bochum, Institut für Experimentalphysik 1, D-44780 Bochum, Germany

⁸University of British Columbia, Vancouver, British Columbia, Canada V6T 1Z1

⁹Brunel University, Uxbridge, Middlesex UB8 3PH, United Kingdom

¹⁰Budker Institute of Nuclear Physics, Novosibirsk 630090, Russia

¹¹University of California at Irvine, Irvine, California 92697, USA

¹²University of California at Riverside, Riverside, California 92521, USA

¹³University of California at San Diego, La Jolla, California 92093, USA

¹⁴University of California at Santa Barbara, Santa Barbara, California 93106, USA

¹⁵University of California at Santa Cruz, Institute for Particle Physics, Santa Cruz, California 95064, USA

¹⁶California Institute of Technology, Pasadena, California 91125, USA

¹⁷University of Cincinnati, Cincinnati, Ohio 45221, USA

¹⁸University of Colorado, Boulder, Colorado 80309, USA

¹⁹Colorado State University, Fort Collins, Colorado 80523, USA

²⁰Technische Universität Dortmund, Fakultät Physik, D-44221 Dortmund, Germany

²¹Technische Universität Dresden, Institut für Kern- und Teilchenphysik, D-01062 Dresden, Germany

²²Laboratoire Leprince-Ringuet, CNRS/IN2P3, Ecole Polytechnique, F-91128 Palaiseau, France

²³University of Edinburgh, Edinburgh EH9 3JZ, United Kingdom

^{24a}INFN Sezione di Ferrara, I-44100 Ferrara, Italy

^{24b}Dipartimento di Fisica, Università di Ferrara, I-44100 Ferrara, Italy

²⁵INFN Laboratori Nazionali di Frascati, I-00044 Frascati, Italy

^{26a}INFN Sezione di Genova, I-16146 Genova, Italy

^{26b}Dipartimento di Fisica, Università di Genova, I-16146 Genova, Italy

²⁷Harvard University, Cambridge, Massachusetts 02138, USA

²⁸Universität Heidelberg, Physikalisches Institut, Philosophenweg 12, D-69120 Heidelberg, Germany

²⁹Humboldt-Universität zu Berlin, Institut für Physik, Newtonstr. 15, D-12489 Berlin, Germany

³⁰Imperial College London, London, SW7 2AZ, United Kingdom

³¹University of Iowa, Iowa City, Iowa 52242, USA

³²Iowa State University, Ames, Iowa 50011-3160, USA

³³Johns Hopkins University, Baltimore, Maryland 21218, USA

- ³⁴*Laboratoire de l'Accélérateur Linéaire, IN2P3/CNRS et Université Paris-Sud 11, Centre Scientifique d'Orsay, B. P. 34, F-91898 Orsay Cedex, France*
- ³⁵*Lawrence Livermore National Laboratory, Livermore, California 94550, USA*
- ³⁶*University of Liverpool, Liverpool L69 7ZE, United Kingdom*
- ³⁷*Queen Mary, University of London, London, E1 4NS, United Kingdom*
- ³⁸*University of London, Royal Holloway and Bedford New College, Egham, Surrey TW20 0EX, United Kingdom*
- ³⁹*University of Louisville, Louisville, Kentucky 40292, USA*
- ⁴⁰*Johannes Gutenberg-Universität Mainz, Institut für Kernphysik, D-55099 Mainz, Germany*
- ⁴¹*University of Manchester, Manchester M13 9PL, United Kingdom*
- ⁴²*University of Maryland, College Park, Maryland 20742, USA*
- ⁴³*University of Massachusetts, Amherst, Massachusetts 01003, USA*
- ⁴⁴*Massachusetts Institute of Technology, Laboratory for Nuclear Science, Cambridge, Massachusetts 02139, USA*
- ⁴⁵*McGill University, Montréal, Québec, Canada H3A 2T8*
- ^{46a}*INFN Sezione di Milano, I-20133 Milano, Italy*
- ^{46b}*Dipartimento di Fisica, Università di Milano, I-20133 Milano, Italy*
- ⁴⁷*University of Mississippi, University, Mississippi 38677, USA*
- ⁴⁸*Université de Montréal, Physique des Particules, Montréal, Québec, Canada H3C 3J7*
- ⁴⁹*Mount Holyoke College, South Hadley, Massachusetts 01075, USA*
- ^{50a}*INFN Sezione di Napoli, I-80126 Napoli, Italy*
- ^{50b}*Dipartimento di Scienze Fisiche, Università di Napoli Federico II, I-80126 Napoli, Italy*
- ⁵¹*NIKHEF, National Institute for Nuclear Physics and High Energy Physics, NL-1009 DB Amsterdam, The Netherlands*
- ⁵²*University of Notre Dame, Notre Dame, Indiana 46556, USA*
- ⁵³*Ohio State University, Columbus, Ohio 43210, USA*
- ⁵⁴*University of Oregon, Eugene, Oregon 97403, USA*
- ^{55a}*INFN Sezione di Padova, I-35131 Padova, Italy*
- ^{55b}*Dipartimento di Fisica, Università di Padova, I-35131 Padova, Italy*
- ⁵⁶*Laboratoire de Physique Nucléaire et de Hautes Energies, IN2P3/CNRS, Université Pierre et Marie Curie-Paris6, Université Denis Diderot-Paris7, F-75252 Paris, France*
- ⁵⁷*University of Pennsylvania, Philadelphia, Pennsylvania 19104, USA*
- ^{58a}*INFN Sezione di Perugia, I-06100 Perugia, Italy*
- ^{58b}*Dipartimento di Fisica, Università di Perugia, I-06100 Perugia, Italy*
- ^{59a}*INFN Sezione di Pisa, I-56127 Pisa, Italy*
- ^{59b}*Dipartimento di Fisica, Università di Pisa, I-56127 Pisa, Italy*
- ^{59c}*Scuola Normale Superiore di Pisa, I-56127 Pisa, Italy*
- ⁶⁰*Princeton University, Princeton, New Jersey 08544, USA*
- ^{61a}*INFN Sezione di Roma, I-00185 Roma, Italy*
- ^{61b}*Dipartimento di Fisica, Università di Roma La Sapienza, I-00185 Roma, Italy*
- ⁶²*Universität Rostock, D-18051 Rostock, Germany*
- ⁶³*Rutherford Appleton Laboratory, Chilton, Didcot, Oxon, OX11 0QX, United Kingdom*
- ⁶⁴*CEA, Irfu, SPP, Centre de Saclay, F-91191 Gif-sur-Yvette, France*
- ⁶⁵*SLAC National Accelerator Laboratory, Stanford, California 94309 USA*
- ⁶⁶*University of South Carolina, Columbia, South Carolina 29208, USA*
- ⁶⁷*Stanford University, Stanford, California 94305-4060, USA*
- ⁶⁸*State University of New York, Albany, New York 12222, USA*
- ⁶⁹*Tel Aviv University, School of Physics and Astronomy, Tel Aviv, 69978, Israel*
- ⁷⁰*University of Tennessee, Knoxville, Tennessee 37996, USA*
- ⁷¹*University of Texas at Austin, Austin, Texas 78712, USA*
- ⁷²*University of Texas at Dallas, Richardson, Texas 75083, USA*
- ^{73a}*INFN Sezione di Torino, I-10125 Torino, Italy*
- ^{73b}*Dipartimento di Fisica Sperimentale, Università di Torino, I-10125 Torino, Italy*
- ^{74a}*INFN Sezione di Trieste, I-34127 Trieste, Italy*
- ^{74b}*Dipartimento di Fisica, Università di Trieste, I-34127 Trieste, Italy*

*Deceased.

†Now at Temple University, Philadelphia, PA 19122, USA.

‡Also with Università di Perugia, Dipartimento di Fisica, Perugia, Italy.

§Also with Università di Roma La Sapienza, I-00185 Roma, Italy.

||Now at University of South Alabama, Mobile, AL 36688, USA.

¶Also with Laboratoire de Physique Nucléaire et de Hautes Energies, IN2P3/CNRS, Université Pierre et Marie Curie-Paris6,

**Also with Università di Sassari, Sassari, Italy.

⁷⁵*IFIC, Universitat de Valencia-CSIC, E-46071 Valencia, Spain*⁷⁶*University of Victoria, Victoria, British Columbia, Canada V8W 3P6*⁷⁷*Department of Physics, University of Warwick, Coventry CV4 7AL, United Kingdom*⁷⁸*University of Wisconsin, Madison, Wisconsin 53706, USA*

(Received 14 July 2009; published 17 December 2009)

We present a search for the radiative leptonic decay $B^+ \rightarrow \ell^+ \nu_\ell \gamma$, where $\ell = e, \mu$, using a data sample of 465×10^6 $B\bar{B}$ pairs collected by the *BABAR* experiment. In this analysis, we fully reconstruct the hadronic decay of one of the B mesons in $Y(4S) \rightarrow B^+ B^-$ decays, then search for evidence of $B^+ \rightarrow \ell^+ \nu_\ell \gamma$ in the rest of the event. We observe no significant evidence of signal decays and report model-independent branching fraction upper limits of $\mathcal{B}(B^+ \rightarrow e^+ \nu_e \gamma) < 17 \times 10^{-6}$, $\mathcal{B}(B^+ \rightarrow \mu^+ \nu_\mu \gamma) < 24 \times 10^{-6}$, and $\mathcal{B}(B^+ \rightarrow \ell^+ \nu_\ell \gamma) < 15.6 \times 10^{-6}$ ($\ell = e$ or μ), all at the 90% confidence level.

DOI: 10.1103/PhysRevD.80.111105

PACS numbers: 13.20.He, 12.38.Qk, 14.40.Nd

The leptonic decay $B^+ \rightarrow \ell^+ \nu_\ell \gamma$ [1], where $\ell = e$ or μ , proceeds via quark annihilation into a virtual W^+ boson with the radiation of a photon. The presence of the photon removes the helicity suppression of the purely leptonic decays, $B^+ \rightarrow \ell^+ \nu_\ell$, although it introduces an additional suppression by a factor of α_{em} . The branching fraction of $B^+ \rightarrow \ell^+ \nu_\ell \gamma$ is predicted to be of order 10^{-6} [2], making it potentially accessible at B factories. The most stringent published limits are from the CLEO Collaboration with $\mathcal{B}(B^+ \rightarrow e^+ \nu_e \gamma) < 2.0 \times 10^{-4}$ and $\mathcal{B}(B^+ \rightarrow \mu^+ \nu_\mu \gamma) < 5.2 \times 10^{-5}$ at the 90% confidence level (C.L.) [3].

The differential branching fraction versus photon energy E_γ involves two form factors, f_V and f_A , which contain the long-distance contribution of the vector and axial currents, respectively, in the $B \rightarrow \gamma$ transition

$$\frac{d\mathcal{B}}{dE_\gamma} = \frac{\alpha_{\text{em}} G_F^2 |V_{ub}|^2}{48\pi^2} m_B^4 \tau_B [f_A^2(E_\gamma) + f_V^2(E_\gamma)] (1-y)y^3, \quad (1)$$

where G_F is the Fermi constant, V_{ub} is the Cabibbo-Kobayashi-Maskawa quark-mixing matrix element describing the coupling of b and u quarks, m_B and τ_B are the B -meson mass and lifetime, respectively, and $y \equiv 2E_\gamma/m_B$. While $f_A = f_V$ in most models [4], some suggest $f_A = 0$ [5]. The branching fraction is given by Ref. [6] as

$$\mathcal{B}(B^+ \rightarrow \ell^+ \nu_\ell \gamma) = \frac{\alpha_{\text{em}} G_F^2 |V_{ub}|^2}{288\pi^2} f_B^2 m_B^5 \tau_B \left(\frac{Q_u}{\lambda_B} - \frac{Q_b}{m_b} \right)^2, \quad (2)$$

where f_B is the B -meson decay constant, $Q_{u,b}$ are the u - and b -quark charges, and m_b is the b -quark mass. The first inverse moment of the B -meson distribution amplitude λ_B is expected to be of order Λ_{QCD} but its theoretical estimation suffers from large uncertainties [7]. It also appears in the branching fractions of two-body hadronic B -meson decays, such as $B \rightarrow \pi\pi$, and plays an important role in QCD factorization [4]. Since there are no hadrons in the final state, an experimental measurement of $B^+ \rightarrow \ell^+ \nu_\ell \gamma$ can provide a clean determination of λ_B .

We present the first search for $B^+ \rightarrow \ell^+ \nu_\ell \gamma$ that exploits the hadronic ‘‘recoil’’ technique, in which one B meson is exclusively reconstructed in a hadronic final state before searching for the signal decay within the rest of the event. This technique improves the handling of event kinematics, providing adequate background suppression without requiring model-dependent constraints on the signal kinematics. Thus, this analysis is valid for all $B \rightarrow \gamma$ form-factor models and over the full kinematic range. This analysis uses a data sample of 465 ± 5 million $B\bar{B}$ pairs, corresponding to an integrated luminosity of 423 fb^{-1} collected at the $Y(4S)$ resonance. The data were recorded with the *BABAR* detector at the asymmetric-energy PEP-II $e^+ e^-$ storage ring at SLAC. The *BABAR* detector is described in detail elsewhere [8].

Signal and background decays are studied using Monte Carlo (MC) samples based on GEANT4 [9]. The simulation includes a detailed model of the *BABAR* detector geometry and response. Beam-related background and detector noise are extracted from data and overlaid on the MC simulations. $Y(4S) \rightarrow B\bar{B}$ signal MC samples are generated with one B meson decaying via $B^+ \rightarrow \ell^+ \nu_\ell \gamma$ using the tree-level model of Ref. [6], which is valid for $y > 0.13$, while the other B meson decays generically. We simulate signal MC samples for two form-factor models, with $f_A = f_V$ and $f_A = 0$, respectively, to evaluate the impact of the decay model on the signal selection efficiency. Large MC samples of generic $B\bar{B}$ and continuum ($e^+ e^- \rightarrow \tau^+ \tau^-$ or $e^+ e^- \rightarrow q\bar{q}$, where $q = u, d, s, c$) events are used to optimize the signal selection criteria. However, the final background estimates are obtained directly from a combination of data and exclusive $B^+ \rightarrow X_u^0 \ell^+ \nu_\ell$ MC samples, where X_u^0 is a neutral meson containing a u quark. The primary background for $B^+ \rightarrow \ell^+ \nu_\ell \gamma$ in this analysis is due to $B^+ \rightarrow X_u^0 \ell^+ \nu_\ell$ decays, with $B^+ \rightarrow \pi^0 \ell^+ \nu_\ell$ ($B^+ \rightarrow \eta \ell^+ \nu_\ell$) comprising approximately 73% (18%) of this semileptonic background. The branching fraction and uncertainty for each $B^+ \rightarrow X_u^0 \ell^+ \nu_\ell$ mode are taken from experimental measurements ($X_u^0 = \pi^0$ [10], ρ [10], η [11], and ω [12]). We assume $\mathcal{B}(B^+ \rightarrow \eta' \ell^+ \nu_\ell) = \mathcal{B}(B^+ \rightarrow \eta \ell^+ \nu_\ell) \times (1 \pm 1)$. We use a light-

cone sum rule model for the η and η' form factors [13] and use the form factor measured in a *BABAR* analysis [14] with the shape parameterization given in Ref. [15] for the π^0 mode.

Event selection begins with the full reconstruction of a charged B meson (B_{tag}) in one of the large number of hadronic final states, $B^- \rightarrow \bar{D}^{(*)} X_{\text{had}}$. We reconstruct the $D^{*-} \rightarrow \bar{D}^0 \pi^-$; $\bar{D}^{*0} \rightarrow \bar{D}^0 \pi^0$, $\bar{D}^0 \gamma$; $D^- \rightarrow K_S^0 \pi^-$, $K_S^0 \pi^- \pi^0$, $K_S^0 \pi^- \pi^- \pi^+$, $K^+ \pi^- \pi^-$, $K^+ \pi^- \pi^- \pi^0$; $\bar{D}^0 \rightarrow K^+ \pi^-$, $K^+ \pi^- \pi^0$, $K^+ \pi^- \pi^- \pi^+$, $K_S^0 \pi^- \pi^+$; and $K_S^0 \rightarrow \pi^- \pi^+$ decay modes. X_{had} is a collection of at most five mesons, composed of both charged and neutral kaons and pions. Well-reconstructed B_{tag} candidates are selected using two kinematic variables: $\Delta E = E_{B_{\text{tag}}} - \sqrt{s}/2$ and $m_{\text{ES}} = \sqrt{s/4 - \vec{p}_{B_{\text{tag}}}^2}$, where $E_{B_{\text{tag}}}$ and $\vec{p}_{B_{\text{tag}}}$ are the energy and momentum of the B_{tag} candidate, respectively, and \sqrt{s} is the total energy of the e^+e^- system, all in the center-of-mass (CM) frame. We require ΔE , which peaks at zero for correctly reconstructed B mesons, to lie between -0.12 and 0.12 GeV or within two standard-deviations from its mean for the given X_{had} mode, whichever is the tighter constraint. We fit the m_{ES} distribution for each X_{had} mode and require that the purity, or fraction of well-reconstructed B mesons, is greater than 12% in the region $m_{\text{ES}} > 5.27$ GeV/ c^2 . If more than one B_{tag} candidate is reconstructed, the one in the highest purity mode is chosen. If there are multiple candidates in this mode, the one that minimizes $|\Delta E|$ is selected.

We define the signal region as $5.27 < m_{\text{ES}} < 5.29$ GeV/ c^2 , since correctly reconstructed B mesons peak in this region near the nominal B -meson mass. The B_{tag} candidates that are incorrectly reconstructed from either continuum events or both B mesons (“combinatoric” events), produce a distribution that is fairly flat below the m_{ES} signal region and decreases within it, as shown in Fig. 1. The shape of the combinatoric distribution is extrapolated into the m_{ES} signal region using MC, while the background contribution from combinatoric events is

estimated directly from the data. To improve the MC estimate of the B_{tag} reconstruction efficiency, we normalize the generic MC to the number of data events that peak within the m_{ES} signal region. Thus, all MC samples are scaled by 90.7%, resulting in good agreement between data and background MC throughout the analysis selection. A charged B_{tag} is reconstructed in about 0.3% of the signal MC events.

Because the two B mesons produced in the $\Upsilon(4S)$ decay have low momenta in the CM frame (0.3 GeV/ c), their decay products are more isotropic than continuum background. For example, $|\cos\theta_{\text{T}}|$, where θ_{T} is the angle in the CM frame between the B_{tag} thrust axis and the thrust axis of all other particles in the event, has a flat distribution for $B\bar{B}$ events and peaks near one for non- $B\bar{B}$ events. The continuum background is suppressed by requiring $\mathcal{L}_B \equiv \prod_i \mathcal{P}_B(x_i) / (\prod_i \mathcal{P}_B(x_i) + \prod_i \mathcal{P}_q(x_i)) > 30\%$, where $\mathcal{P}_B(x_i)$ ($\mathcal{P}_q(x_i)$) are probability density functions determined from MC that describe $B\bar{B}$ (continuum) events for the five event-shape variables x_i . The variables used are: the ratio of the second to zeroth Fox-Wolfram moment [16] computed using all charged and neutral particles in the event, the cosine of the angle between $\vec{p}_{B_{\text{tag}}}$ and the beam axis, the magnitude of the B_{tag} thrust, the component of the B_{tag} thrust along the beam axis, and $|\cos\theta_{\text{T}}|$. This requirement improves the agreement between data and MC by suppressing unmodeled continuum backgrounds, such as $e^+e^- \rightarrow e^+e^-\ell^+\ell^-$ via two photons.

In the sample of selected B_{tag} candidates, we identify events in which the remaining tracks, calorimeter clusters, and missing momentum vector (\vec{p}_{miss}) are consistent with $B^+ \rightarrow \ell^+ \nu_{\ell} \gamma$ candidates. We select events with exactly one track, which reduces the signal efficiency by 25% but removes over 99% of the simulated background events with a reconstructed B_{tag} . This signal track is required to have a charge opposite to that of the B_{tag} , to satisfy particle identification (PID) criteria for either a muon or electron, and to be inconsistent with a kaon hypothesis. In the electron mode, the four-momenta of signal tracks are re-defined to include those of any bremsstrahlung photon candidates. Such a candidate is defined as any cluster whose momentum vector, when compared to that of the signal track (\vec{p}_{ℓ}), is separated by $|\Delta\theta| < 3^\circ$ and $-3^\circ < Q_e \times \Delta\phi < 13^\circ$, where $Q_e = \pm 1$ is the e^\pm charge and θ (ϕ) is the polar (azimuthal) angle relative to the beam axis, in the lab frame. Finally, the signal photon candidate is chosen as the cluster with the highest CM energy, excepting bremsstrahlung photon candidates.

We significantly reduce the background by requiring that the kinematics of the signal track and photon candidate are consistent with the existence of a third massless particle originating from the signal B meson. To do this, we use the four-momentum of the expected signal B meson (p_B), which is assigned an energy of $\sqrt{s}/2$, a momentum vector pointing along $-\vec{p}_{B_{\text{tag}}}$, and the nominal B -meson mass. The

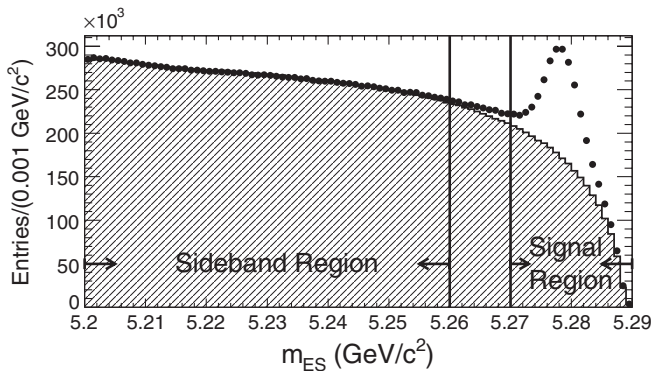


FIG. 1. m_{ES} distribution, after B_{tag} reconstruction and continuum suppression, of data (points) and the expected combinatoric background as predicted by the MC (shaded).

neutrino mass squared is then defined as $m_\nu^2 \equiv (p_B - p_\ell - p_\gamma)^2$, where p_ℓ (p_γ) is the four-momentum of the signal track (photon candidate). As shown in Fig. 2, the background increases with m_ν^2 , while $B^+ \rightarrow \ell^+ \nu_\ell \gamma$ events peak at $m_\nu^2 = 0$ with an enhanced tail in the electron mode due to unrecovered bremsstrahlung photons. We require $-1 < m_\nu^2 < 0.46$ (0.41) GeV^2/c^4 for the electron (muon) modes. In addition, the lepton and neutrino should be emitted back-to-back in the rest frame that recoils from the photon emission, defined as $p_B - p_\gamma$. We require $\cos\theta_{\ell\nu} < -0.93$ in this frame, where $\theta_{\ell\nu}$ is the angle between \vec{p}_ℓ and \vec{p}_{miss} . After all other selection criteria are applied, the MC indicates that m_ν^2 and $\cos\theta_{\ell\nu}$ together remove 99% of background events with a 30 and 20% reduction in the signal efficiency for the electron and muon modes, respectively.

The dominant backgrounds are due to $B^+ \rightarrow \pi^0 \ell^+ \nu_\ell$ ($\eta \ell^+ \nu_\ell$) events in which π^0 (η) $\rightarrow \gamma\gamma$ fakes the $B^+ \rightarrow \ell^+ \nu_\ell \gamma$ signal photon. To suppress this background, we reject events containing a π^0 (η) candidate, reconstructed using the signal photon candidate and a second cluster having CM energy E_{γ_2} . For π^0 candidates, we require a $\gamma\gamma$ invariant mass between 120–145 MeV/c^2 with $E_{\gamma_2} > 30$ MeV or between 100–160 MeV/c^2 with $E_{\gamma_2} >$

80 MeV. For η candidates, we require a $\gamma\gamma$ invariant mass between 515–570 MeV/c^2 with $E_{\gamma_2} > 100$ MeV. Likewise, $B^+ \rightarrow \omega \ell^+ \nu_\ell \rightarrow [\pi^0 \gamma] \ell^+ \nu_\ell$ events are suppressed by rejecting any event in which the signal photon candidate and a π^0 candidate produce an invariant mass between 730–830 MeV/c^2 . This π^0 candidate is defined as any two clusters with CM energy > 70 MeV which produce a $\gamma\gamma$ invariant mass between 115–145 MeV/c^2 . After applying all other selection criteria, these vetoes reduce the $B^+ \rightarrow \pi^0 \ell^+ \nu_\ell$ and $B^+ \rightarrow X_u^0 \ell^+ \nu_\ell$ background events, with $X_u^0 \neq \pi^0$, by 65% and 50%, respectively. Finally, we require the lateral moment [17] of the calorimeter energy deposit for the signal photon candidate, which peaks at 25% for single photons, to be between 0 and 55%. This suppresses $B^+ \rightarrow \pi^0 \ell^+ \nu_\ell$ events in which the two photons from the π^0 decay are reconstructed as a single merged photon.

Once the B_{tag} , signal photon, and lepton are identified, $B^+ \rightarrow \ell^+ \nu_\ell \gamma$ events are expected to contain little or no additional energy within the calorimeter. However, additional energy deposits can result from hadronic shower fragments, beam-related photons, and photons from unreconstructed $\bar{D}^* \rightarrow \bar{D} \gamma / \pi^0$ transitions in the B_{tag} candidate. The total energy of all additional clusters is required to be less than 0.8 GeV, counting only clusters with lab-frame energy greater than 50 MeV. We also require that \vec{p}_{miss} points within the fiducial acceptance of the detector.

To avoid experimenter bias, we optimize all the selection criteria and determine the number of expected background events in the signal region (N_ℓ^{bkg}), for $\ell = e$ or μ , before looking at any data events selected by the criteria. We optimize by maximizing the figure of merit $\varepsilon_\ell^{\text{sig}} / (\frac{1}{2} n_\sigma + \sqrt{N_\ell^{\text{bkg}}})$ [18], where $n_\sigma = 1.3$ and $\varepsilon_\ell^{\text{sig}}$ is the total signal efficiency including that of the B_{tag} reconstruction. The signal branching fraction is calculated using $\mathcal{B}_\ell = (N_\ell^{\text{obs}} - N_\ell^{\text{bkg}}) / \varepsilon_\ell^{\text{sig}} N_{B^\pm}$, where $N_{B^\pm} = 465 \times 10^6$ is the number of B^\pm mesons in the data sample and N_ℓ^{obs} is the number of data events within the signal region.

To verify the modeling of $\varepsilon_\ell^{\text{sig}}$, we remove the $B^+ \rightarrow X_u^0 \ell^+ \nu_\ell$ vetoes, select events containing a π^0 candidate, and substitute the π^0 in place of the signal photon candidate. The resulting m_ν^2 distribution from $B^+ \rightarrow \pi^0 \ell^+ \nu_\ell$ is expected to resemble that of the signal. We observe a peak in the data that agrees with MC expectations within the 15% statistical uncertainty of the data, as shown in Fig. 3. For cross-check purposes only, we determine the $B^+ \rightarrow \pi^0 \ell^+ \nu_\ell$ efficiency using an exclusive $B^+ \rightarrow \pi^0 \ell^+ \nu_\ell$ MC sample and the background contribution using generic MC. The peak in data corresponds to $\mathcal{B}(B^+ \rightarrow \pi^0 \ell^+ \nu_\ell) = (7.8_{-1.1}^{+1.7}) \times 10^{-5}$, where the uncertainty is statistical. This branching fraction is consistent with the current world-average value of $(7.7 \pm 1.2) \times 10^{-5}$ [10], which is also the value used in the MC samples.

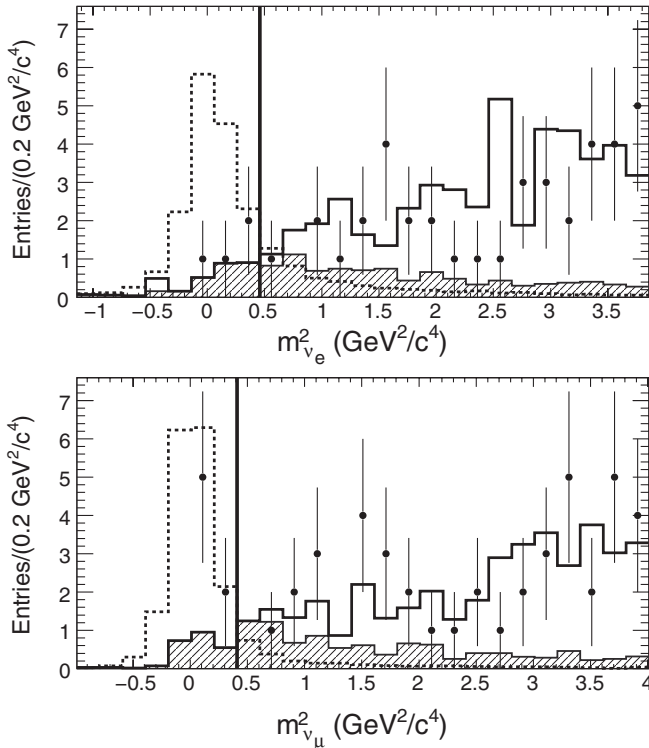


FIG. 2. m_ν^2 distribution after all selection criteria are applied, in electron (top) and muon (bottom) modes for the m_{ES} peaking (shaded) plus nonpeaking (solid) contributions in the full background MC sample, signal MC normalized to $\mathcal{B} = 40 \times 10^{-6}$ (dashed), and data (points). Events to the left of the vertical lines are selected. N_ℓ^{comb} of Table I is determined from sideband data, not from the MC shown here.

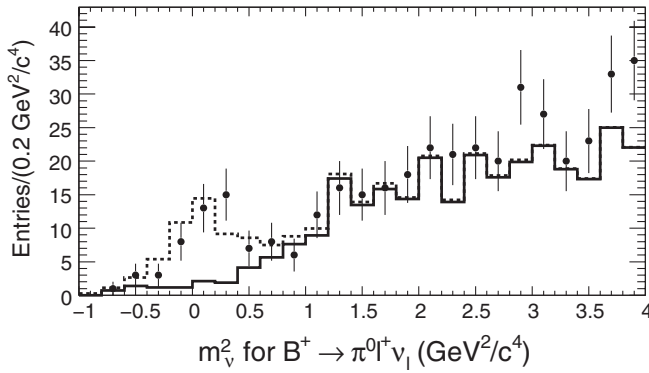


FIG. 3. m_ν^2 distribution for $B^+ \rightarrow \pi^0 \ell^+ \nu_\ell$ ($\ell = e$ and μ), using the procedure described in the text where γ is substituted with a π^0 candidate, of data (points) and of $B^+ \rightarrow \pi^0 \ell^+ \nu_\ell$ MC normalized to $\mathcal{B} = 7.7 \times 10^{-5}$ (dashed) and added to the expected background (solid).

The total number of background events N_ℓ^{bkg} has two components: N_ℓ^{peak} the number of expected background events having a correctly reconstructed B_{tag} and hence peaking within the m_{ES} signal region, and N_ℓ^{comb} the number of expected combinatoric background events, including both $B\bar{B}$ and continuum events. The m_ν^2 and $\cos\theta_{\ell\nu}$ restrictions ensure kinematic and topological consistency with a three-body decay involving a massless and undetected particle: the neutrino. By further requiring that exactly one track recoils from a fully-reconstructed B_{tag} , lepton number and PID ensures the track is a lepton. Thus, only $B^+ \rightarrow \ell^+ \nu_\ell \gamma$ decays can peak within the signal region, unless the signal photon candidate actually arises from one or more particles that mimic the kinematics of $B^+ \rightarrow \ell^+ \nu_\ell \gamma$, which only occurs in specific pathological $B^+ \rightarrow X_u^0 \ell^+ \nu_\ell$ decays. Therefore, we determine N_ℓ^{peak} using exclusive $B^+ \rightarrow X_u^0 \ell^+ \nu_\ell$ MC simulations and validate the lack of additional peaking backgrounds with generic MC. Other decay modes passing the selection criteria do so with poorly reconstructed B_{tag} candidates and thus produce a combinatoric distribution in m_{ES} . We determine N_ℓ^{comb} from an extrapolation of the observed number of data events within the m_{ES} sideband region, defined as $5.20 < m_{\text{ES}} < 5.26 \text{ GeV}/c^2$. We observe 1 (4) data events within the m_{ES} sideband for the electron (muon) mode.

The uncertainty on N_ℓ^{comb} is dominated by the sideband data statistics. It also includes the systematic uncertainty from the combinatoric background shape, estimated by varying the selection criteria and the method used to extrapolate this shape (14.6%). The error on N_ℓ^{peak} is dominated by uncertainties in the branching fractions and form factors associated with the various exclusive $B^+ \rightarrow X_u^0 \ell^+ \nu_\ell$ decays (13.6%). Additional systematic uncertainties result from MC modeling of the data efficiency, which we apply to both N_ℓ^{peak} and $\varepsilon_\ell^{\text{sig}}$: electron PID (0.9%) or muon PID (1.3%), \mathcal{L}_B (1.4%), m_ν^2 (0.5% for $\varepsilon_\ell^{\text{sig}}$, 1.4% for

N_ℓ^{peak}), and the reconstructions of the track (0.4%), photon (1.8%), and B_{tag} (3.1%). The last of these, which also accounts for uncertainty in N_{B^\pm} , is estimated by varying the shape of the m_{ES} combinatoric distribution and the size of the m_{ES} signal and sideband regions.

Branching fraction limits and uncertainties are computed using the frequentist formalism of Feldman and Cousins [19], with the uncertainties on N_ℓ^{bkg} and $\varepsilon_\ell^{\text{sig}}$ modeled using Gaussian distributions. Since $\mathcal{B}(B^+ \rightarrow \ell^+ \nu_\ell \gamma)$ is expected to be independent of the lepton type, we also combine the two modes by maximizing a likelihood function defined as the product of both Poisson probabilities in N_ℓ^{bkg} , where \mathcal{B}_ℓ is the mean.

We observe 4 (7) data events within the signal region for the electron (muon) mode, compared to an expected background of 2.7 ± 0.6 (3.4 ± 0.9) events. This corresponds to a signal significance of 1.2σ (1.8σ), a combined significance of 2.1σ , and the results given in Table I. The effective detector and PID thresholds are about 20 MeV for photon energy and 400 (800)MeV/c for electron (muon) momentum, and we apply no minimum energy requirements. Thus, this analysis is essentially independent of the kinematic model; we assume the $f_A = f_V$ signal model, but the $f_A = 0$ model yields consistent $\varepsilon_\ell^{\text{sig}}$ values. Since certain theoretical calculations are most reliable at high E_γ [7], we also report a partial branching fraction limit $\Delta\mathcal{B}$ by selecting events with a photon candidate energy greater than 1 GeV, which reduces $\varepsilon_\ell^{\text{sig}}$ by 30%. We observe 2 (4) data events with $N_\ell^{\text{bkg}} = 1.4 \pm 0.3$ (2.5 ± 1.0), resulting in $\Delta\mathcal{B}(B^+ \rightarrow \ell^+ \nu_\ell \gamma) < 14 \times 10^{-6}$ at 90% C.L.

In Table I, we also report model-specific limits by introducing a kinematic requirement on the relationship between $\cos\theta_{\gamma\ell}$ and $\cos\theta_{\gamma\nu}$, where $\theta_{\gamma\ell}$ ($\theta_{\gamma\nu}$) is the angle between the photon candidate momentum and \vec{p}_ℓ (\vec{p}_{miss}) in the signal B rest frame. The photon is emitted preferentially back-to-back with the lepton in the $f_A = f_V$ model, and with either the lepton or neutrino when $f_A = 0$. Thus, we require $(\cos\theta_{\gamma\ell} - 1)^2 + (\cos\theta_{\gamma\nu} + 1)^2/3 > 0.4$ or $(\cos\theta_{\gamma\nu} - 1)^2 + (\cos\theta_{\gamma\ell} + 1)^2/3 > 0.4$ for the $f_A = 0$ model, and only the former relationship for $f_A = f_V$. This reduces $\varepsilon_\ell^{\text{sig}}$ in both modes and models by 40%. We observe 0 (0) data events in the electron (muon) mode with $N_\ell^{\text{bkg}} = 0.6 \pm 0.1$ (1.0 ± 0.4) for the $f_A = f_V$ model, and 3 (2) data events with $N_\ell^{\text{bkg}} = 1.2 \pm 0.4$ (1.5 ± 0.6) for $f_A = 0$.

In conclusion, we have searched for $B^+ \rightarrow \ell^+ \nu_\ell \gamma$ using a hadronic recoil technique and observe no significant signal within a data sample of $465 \times 10^6 B\bar{B}$ pairs. We present model-specific branching fraction limits in Table I. We also report a model-independent limit of $\mathcal{B}(B^+ \rightarrow \ell^+ \nu_\ell \gamma) < 15.6 \times 10^{-6}$ at the 90% C.L., which is consistent with the standard model prediction and is the most

TABLE I. Expected background yields $N_\ell^{\text{bkg}} = N_\ell^{\text{comb}} + N_\ell^{\text{peak}}$, signal efficiencies $\varepsilon_\ell^{\text{sig}}$, number of observed data events N_ℓ^{obs} , resulting branching fraction limits at 90% C.L., and the combined central value $\mathcal{B}_{\text{combined}}$. Model-specific limits are also presented. Uncertainties are given as statistical \pm systematic.

	$B^+ \rightarrow e^+ \nu_e \gamma$	$B^+ \rightarrow \mu^+ \nu_\mu \gamma$	$B^+ \rightarrow \ell^+ \nu_\ell \gamma$
N_ℓ^{comb}	$0.3 \pm 0.3 \pm 0.1$	$1.2 \pm 0.6 \pm 0.6$	
N_ℓ^{peak}	$2.4 \pm 0.3 \pm 0.4$	$2.1 \pm 0.3 \pm 0.3$	
N_ℓ^{bkg}	$2.7 \pm 0.4 \pm 0.4$	$3.4 \pm 0.7 \pm 0.7$	
$\varepsilon_\ell^{\text{sig}}$	$(7.8 \pm 0.1 \pm 0.3) \times 10^{-4}$	$(8.1 \pm 0.1 \pm 0.3) \times 10^{-4}$	
N_ℓ^{obs}	4	7	
$\mathcal{B}_{\text{combined}}$			$(6.5^{+7.6+2.8}_{-4.7-0.8}) \times 10^{-6}$
Model-independent limits	$<17 \times 10^{-6}$	$<26 \times 10^{-6}$	$<15.6 \times 10^{-6}$
$f_A = f_V$ limits	$<8.4 \times 10^{-6}$	$<6.7 \times 10^{-6}$	$<3.0 \times 10^{-6}$
$f_A = 0$ limits	$<29 \times 10^{-6}$	$<22 \times 10^{-6}$	$<18 \times 10^{-6}$

stringent published upper limit to date. Using Eq. (2) with $f_B = 0.216 \pm 0.022$ GeV [20], $m_B = 5.279$ GeV/ c^2 , $\tau_B = 1.638$ ps, $m_b = 4.20$ GeV/ c^2 , and $|V_{ub}| = (3.93 \pm 0.36) \times 10^{-3}$ [10], the combined branching fraction likelihood function corresponds to a limit of $\lambda_B > 0.3$ GeV at the 90% C.L.

We are grateful for the excellent luminosity and machine conditions provided by our PEP-II colleagues, and for the substantial dedicated effort from the computing organiza-

tions that support *BABAR*. The collaborating institutions wish to thank SLAC for its support and kind hospitality. This work is supported by the DOE and NSF (USA), NSERC (Canada), CEA and CNRS-IN2P3 (France), BMBF and DFG (Germany), INFN (Italy), FOM (The Netherlands), NFR (Norway), MES (Russia), MEC (Spain), and STFC (United Kingdom). Individuals have received support from the Marie Curie EIF (European Union) and the A. P. Sloan Foundation.

-
- [1] Charge conjugation is implied throughout this paper.
 - [2] Y.-Y. Charng and H. Li, Phys. Rev. D **72**, 014003 (2005).
 - [3] T.E. Browder *et al.* (CLEO Collaboration), Phys. Rev. D **56**, 11 (1997).
 - [4] E. Lunghi, D. Pirjol, and D. Wyler, Nucl. Phys. **B649**, 349 (2003); S. Descotes-Genon and C.T. Sachrajda, Nucl. Phys. **B650**, 356 (2003).
 - [5] G. Burdman, T. Goldman, and D. Wyler, Phys. Rev. D **51**, 111 (1995).
 - [6] G.P. Korchemsky, D. Pirjol, and T.M. Yan, Phys. Rev. D **61**, 114510 (2000).
 - [7] P. Ball and E. Kou, J. High Energy Phys. 04 (2003) 029.
 - [8] B. Aubert *et al.* (*BABAR* Collaboration), Nucl. Instrum. Methods Phys. Res., Sect. A **479**, 1 (2002).
 - [9] S. Agostinelli *et al.* (GEANT4 Collaboration), Nucl. Instrum. Methods Phys. Res., Sect. A **506**, 250 (2003).
 - [10] C. Amsler *et al.* (Particle Data Group), Phys. Lett. B **667**, 1 (2008).
 - [11] B. Aubert *et al.* (*BABAR* Collaboration), Phys. Rev. Lett. **101**, 081801 (2008).
 - [12] C. Schwanda *et al.* (Belle Collaboration), Phys. Rev. Lett. **93**, 131803 (2004).
 - [13] P. Ball and R. Zwicky, Phys. Rev. D **71**, 014015 (2005).
 - [14] B. Aubert *et al.* (*BABAR* Collaboration), Phys. Rev. Lett. **98**, 091801 (2007).
 - [15] D. Becirevic and A.B. Kaidalov, Phys. Lett. B **478**, 417 (2000).
 - [16] G.C. Fox and S. Wolfram, Phys. Rev. Lett. **41**, 1581 (1978).
 - [17] A. Drescher *et al.* (ARGUS Collaboration), Nucl. Instrum. Methods Phys. Res., Sect. A **237**, 464 (1985).
 - [18] G. Punzi, in *Proceedings of the Conference on Statistical Problems in Particle Physics, Astrophysics, and Cosmology, Stanford, 2003*, edited by L. Lyons, R. Mount, and R. Reitmeyer, eConf C030908, MODT002 (2003).
 - [19] G.J. Feldman and R.D. Cousins, Phys. Rev. D **57**, 3873 (1998).
 - [20] A. Gray *et al.* (HPQCD Collaboration), Phys. Rev. Lett. **95**, 212001 (2005).